ELSEVIER

Journal of Nuclear Materials 307–311 (2002) 1215–1220

journal of nuclear materials

www.elsevier.com/locate/jnucmat

Highly thermal conductive, sintered SiC fiber-reinforced 3D-SiC/SiC composites: experiments and finite-element analysis of the thermal diffusivity/conductivity

R. Yamada *, N. Igawa, T. Taguchi, S. Jitsukawa

Department of Materials Science and Technology, Japan Atomic Energy Research Institute, Tokai-mura, Naka-gun, Ibaraki-ken 319-1195, Japan

Abstract

Chemical vapor infiltrated (CVI) and polymer impregnated and pyrolized (PIP) SiC/SiC composites were fabricated by using highly thermal conductive, sintered SiC fiber. These composites had relatively high thermal diffusivity/conductivity values, which were two or three times larger than those reinforced with Hi-Nicalon or Hi-Nicalon Type S fibers. The improvement of thermal diffusivity by using this fiber was more noticeable for PIP composites than for CVI composites. A 2D finite element thermal analysis supported the experimental results, and revealed that highly thermal conductive SiC fiber was much effective for PIP composites and that the increase of fiber volume worsened CVI composite thermal diffusivity if low thermal conductive SiC fibers were used.

1. Introduction

SiC fiber-reinforced SiC composites (SiC/SiC) have been proposed for an advanced structural material for reactor-blanket modules [1–4]. To reduce thermal stresses in blanket walls lower than an allowable design stress, relatively high thermal conductivity is a requisite property for SiC/SiC composites. For example, the design of DREAM reactor proposed by JAERI [1,2] requires at least 15 $W\,m^{-1}\,K^{-1}$ for the neutron-irradiated first wall of a blanket whose allowable design stress is set to 200 MPa. When the degradation of thermal conductivity due to irradiation is taken into account, most data acquired so far indicate that the requirement is not satisfied for the cases of chemical vapor infiltrated (CVI) or polymer impregnated and pyrolized (PIP) composites [3–7]. The recently developed sintered SiC fiber, which contains Al additive (<0.6 wt%) for enhancing both sintering and grain growth, has very high thermal conductivity [8–11]. In this paper, we have studied how sintered SiC fiber improves the overall thermal diffusivity/conductivity of 3D SiC/SiC composites made with the CVI or the PIP method. In addition, we have performed 2D thermal analysis with a finite element method (FEM) for elucidating the experimental results and testing the effect of varying the thermal conductivity values for the fiber and matrix constituents on the composite thermal diffusivity.

2. Experimental

3D fabric preforms, named as Tyranno™ SAC fabrics, were woven from amorphous Si–Al–C–O fiber (Tyranno™ AM fiber, 10 μm diameter) by Ube Industries. After weaving, they were sintered at a high temperature (over 1900 °C). The heat treatment was identical to the heat treatment used to convert AM fiber into SA fiber, which has thermal conductivity >60 $W\,m^{-1}\,K^{-1}$ at RT [9,10]. The above procedures were employed to enable weaving of the low tensile modulus AM fiber. Similar procedures were adopted for sintered

* Corresponding author. Tel.: +81-29 282 5403; fax: +81-29 282 6556.

E-mail address: reiji@popsvr.tokai.jaeri.go.jp (R. Yamada).

0022-3115/02/$ - see front matter
PII: S0022-3115(02)00957-1

Table 1
Bulk density, fiber volume and porosity values of 3D CVI and PIP SiC/SiC composites

	CVI SiC/SiC			PIP SiC/SiC		
	$X:Y:Z = 1:1:0.2$ (●○▽▼)	$X:Y:Z = 1:1:1$ (□■)	$X:Y:Z = 1:1:4$ (◇◆)	$X:Y:Z = 1:1:0.2$ (●○▽▼)	$X:Y:Z = 1:1:1$ (□■)	$X:Y:Z = 1:1:4$ (◇◆)
Bulk density ($g\,cm^{-3}$)	2.85	2.67	2.89	2.57	2.18	2.33, 2.30
Fiber volume (%)	31	37	23	34	37	23
Porosity (%)	10	14	8	13	27	21

SiC fiber-bonded ceramic, which only consists of hexagonal columnar fibers [10,11].

SiC/SiC composites were fabricated by either the CVI or the PIP method. The fiber $X:Y:Z$ configurations were nominally 1:1:0.2, 1:1:1, 1:1:4, where the Z-direction was taken through the thickness of a specimen. Mitsui Engineering & Shipbuilding Co., Ltd. performed the CVI-method at 1200 °C, and Kawasaki Heavy Industries Ltd. performed the PIP-method, where six cycles of impregnated polycarbosilane (PCS) were pyrolyzed at 1000 °C followed by the final heat treatment at 1200 °C. The bulk density, fiber volume and porosity values for each fiber configuration and fabrication method are listed in Table 1. Carbon coating between fiber and matrix to improve mechanical properties was not carried out for both CVI and PIP. For the PIP, SiC CVD coating on fibers was performed to protect them from chemical reactants produced during PIP process.

Thermal diffusivity of a specimen (nominally 10 mm in diameter and 3 mm in thickness) was measured in vacuum using the laser flash method (PS-2000, Rigaku Co., Ltd.). The transient temperature response at the rear surface of a specimen was monitored with an IR detector whose sensitive area's diameter was about 8 mm. The through-the-thickness thermal diffusivity (α) was determined from $\alpha = 0.1388L^2/t_{1/2}$ [12], where $t_{1/2}$ is the time required to reach half of the total temperature rise on the rear surface of a specimen, and L is the specimen thickness in the Z-direction. Thermal conductivity was calculated by $\alpha C_p \rho$, where C_p and ρ are the specific heat and the bulk density, respectively. The specific heat of monolithic SiC [13] was used for the SiC/SiC composites since a small amount of impurities and/or additives gives a minor effect on the overall specific heat, which is also considered relatively insensitive to composite structures. Some specimens were double-checked by using a different another laser flash system (TC-2000, Shinku-Rico Inc.).

3. 2D finite element method

To simulate the laser flash thermal diffusivity measurement, a 2D thermal analysis was performed by using the FEM code, ABAQUS (Hibbitt, Karlsson & Sorensen, Inc.). A rectangular geometry (10×3 mm) was meshed with 8-node quadrilateral elements. The front boundary of the geometry was set to receive a 1 ms heat pulse of 10^8 $W\,m^{-2}$, which was experimentally equivalent to about 8 J laser power incident on a 10 mm diameter disc for 1 ms. The heat flux at the rear boundary was governed by radiation whose emissivity was postu-

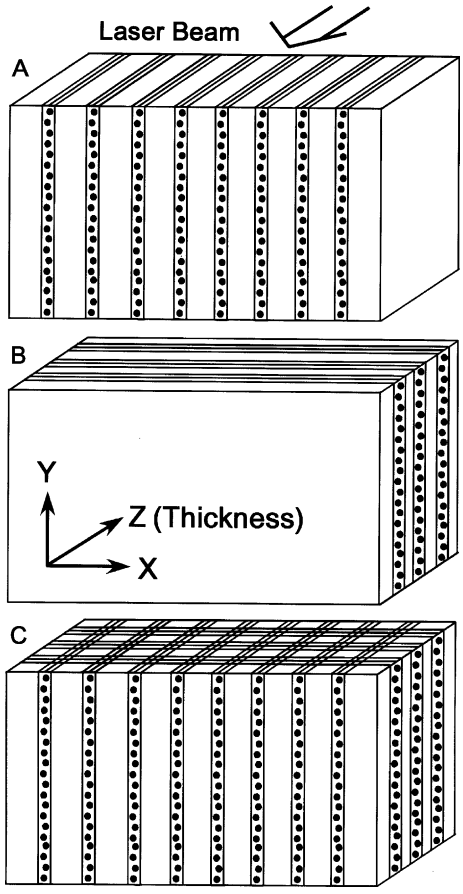

Fig. 1. Schematic diagram of fiber configurations. In thermal diffusivity measurement the laser beam is incident on specimens along the Z-direction. Top surfaces (XZ plane) of A, B, and C are meshed for 2D FEM, corresponding to 1D (Z-direction: through-the-thickness), 2D (XY plane), and 3D fiber configurations, respectively.

lated 0.5. At the two side boundaries, adiabatic or radiative condition was selected. However, no noticeable differences were exhibited by either condition. Thermal diffusivity was calculated from the $t_{1/2}$-value derived from a temperature rise curve, which was obtained at each time step by plotting the temperature averaged between regions of ±4 mm from the center at the rear boundary, which corresponded to the sensitive area of the IR detector.

Fig. 1 depicts three fiber configurations. For configurations A and B, the thermo-physical properties for three different fibers (Tyranno SA™ [9,10], and Hi-Nicalon™ and Hi-Nicalon™ Type S [14]) were selected for studying the effect of fiber volume, configuration, and thermal conductivity on overall composite thermal diffusivity. The configuration C will help us to understand the experimental results.

4. Results and discussion

Figs. 2 and 3 illustrate the measured thermal diffusivity/conductivity values for 3D-CVI and PIP SiC/SiC composites (see Table 1). For fiber configuration $X{:}Y{:}Z = 1{:}1{:}0.2$, the thermal diffusivities at RT and 600 °C were measured with a second laser flash system for double checking. The data were in good agreement.

In Fig. 2, 3D-CVI SiC/SiC composites with fiber configurations $X{:}Y{:}Z = 1{:}1{:}0.2$ and 1:1:4 had higher thermal diffusivity and conductivity than that with $X{:}Y{:}Z = 1{:}1{:}1$. The highest conductivity value was more than 60 $\mathrm{W\,m^{-1}\,K^{-1}}$ at RT and about 36–28 $\mathrm{W\,m^{-1}\,K^{-1}}$ in the region of 600–1000 °C, which are relatively high (nearly two times) compared with 2D-CVI SiC/SiC composites reinforced with other SiC fibers [3–7]. The high values are comparable to those of sintered SiC fiber-bonded ceramics synthesized by hot-pressing [10,11].

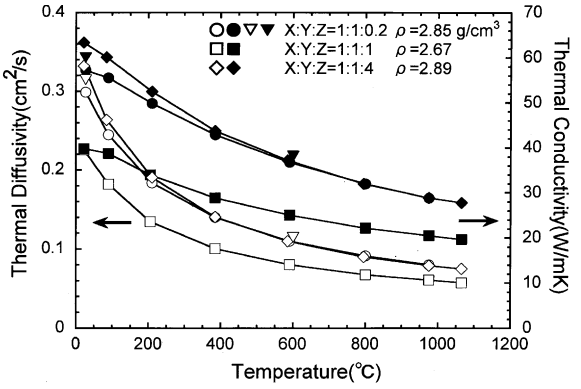

Fig. 2. Through-the-thickness thermal diffusivity/conductivity of CVI SiC/SiC composites reinforced with 3D Tyranno SAC fabrics: ○□◇ thermal diffusivity; ●■◆ thermal conductivity. The data double-checked by other equipment are also shown (▽, ▼) in fiber configuration $X{:}Y{:}Z = 1{:}1{:}0.2$. Refer to Table 1 for pertinent density, fiber volume and porosity data.

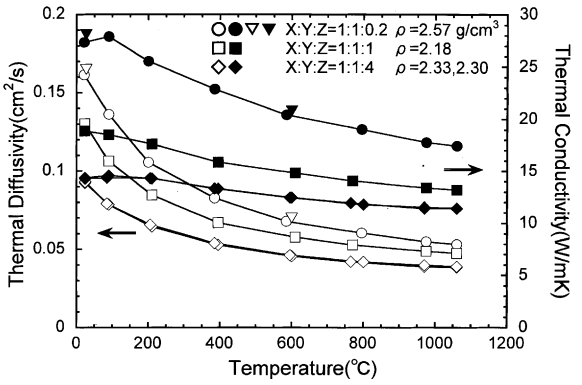

Fig. 3. Through-the-thickness thermal diffusivity/conductivity of PIP SiC/SiC composites reinforced with 3D Tyranno SAC fabrics: ○□◇ thermal diffusivity; ●■◆ thermal conductivity. The data double-checked by other equipment are also shown (▽, ▼) in fiber configuration $X{:}Y{:}Z = 1{:}1{:}0.2$. Refer to Table 1 for pertinent density, fiber volume and porosity data.

In Fig. 3, 3D-PIP SiC/SiC composite with fiber configuration $X{:}Y{:}Z = 1{:}1{:}0.2$ had the highest thermal diffusivity and conductivity (more than 25 $\mathrm{W\,m^{-1}\,K^{-1}}$ at room temperature and about 20–17 $\mathrm{W\,m^{-1}\,K^{-1}}$ in the region of 600–1000 °C). Similar to 3D-CVI SiC/SiC composites, these values are also very high (nearly three times) compared with those of conventional 2D-PIP SiC/SiC composites [3–7].

Fig. 4 shows the calculated results at 600 °C for simulating the experimental results of Figs. 2 and 3 by using the 3D-fiber configuration of Fig. 1(C). Fiber and matrix density values as well as thermal conductivity values necessary for the input data of the FEM calculations were listed in Table 2. Since radial and axial thermal conductivities of the fibers were assumed to be identical and thereby both X- and Y-directional fibers would have the same effect on the Z-directional heat flow, the experimental 3D fiber configurations were converted to the computational 2D ones in the XZ plane of Fig. 1(C). For instance, $X{:}Y{:}Z = 1{:}1{:}0.2$, 1:1:1, and 1:1:4 were converted to $X{:}Z = 2{:}0.2$, 2:1, and 2:4, respectively.

For the case of CVI composites, the calculated and experimental results agreed fairly well when a higher matrix thermal conductivity was used together with a higher matrix density. For the case of PIP composites, several matrix thermal conductivity values at 600 °C were tested to search for a better agreement. However, the agreement was acceptable only for $X{:}Y{:}Z = 1{:}1{:}0.2$ with the matrix density of 2.38 $\mathrm{g\,cm^{-3}}$ when using a matrix thermal conductivity of 15 $\mathrm{W\,m^{-1}\,K^{-1}}$.

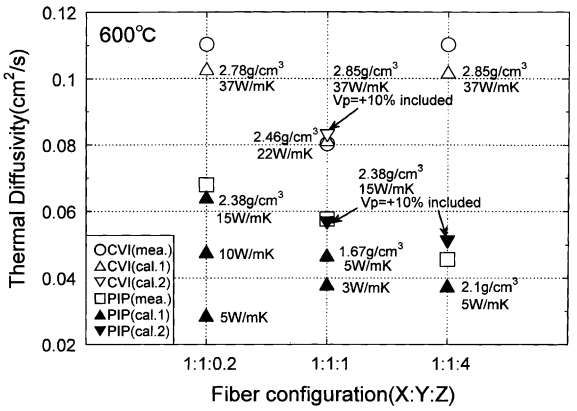

Fig. 4. Comparison between calculated and experimental results of through-the-thickness thermal diffusivity for 3D CVI and PIP SiC/SiC composites at 600 °C. Input data for matrix density and thermal conductivity values are noted in the figure for calculation in each case (cal. 1). In addition, porosity (V_p), was taken into account in some cases (cal. 2).

A previous study indicated that flat shape cavities significantly decreased the thermal conductivity of SiC/SiC composites [15]. For specimens with porosity more than 10% (see Table 1), we calculated thermal diffusivity values under the conditions of rectangular-shaped cavities distributed in the matrices with the highest density and thermal conductivity values. The calculated results for the 10% increase in porosity are also added in Fig. 4 (cal. 2). The experimental and calculated results agreed fairly well when this porosity correction was applied. The 10% increase in porosity was comparable to the difference in porosity between corrected and uncorrected specimens. Apparently the porosity significantly hindered the Z-directional heat flow.

The models of Fig. 1(A) (1D model) and B (2D model) were suitable for checking the effect of fiber configuration and fiber volume on the through-the-thickness thermal conductivity, and the calculated results would give us some insight into tailoring composite thermal conductivity not only for 1D, 2D but also for 3D SiC/SiC composites. Figs. 5 and 6 show calculated results for CVI and PIP SiC/SiC composites at 600 °C, respectively. For the CVI case, the fiber volume of Tyranno SA did not affect the composite thermal diffusivity, whereas for Hi-Nicalon and Type S fibers the thermal diffusivity was reduced with increasing fiber volume. Apparently when the 2D (XY) sheets were made of lower thermal conductive fibers, Z-directional thermal diffusivity was more reduced than that for 1D (Z) fibers. It should be reasonable since the total area of 1D fibers normal to Z-direction was smaller than the corresponding area of the XY sheets, which directly caused to reduce the Z-directional thermal diffusion.

For the PIP composites, both 5 and 15 $W\,m^{-1}\,K^{-1}$ for matrix thermal conductivity at 600 °C were used for the input data. High thermal conductive Tyranno fiber increased through-the-thickness thermal diffusivity with increasing fiber volume, especially for 1D fibers configured to Z-direction. However, for the cases of Hi-Nicalon or Hi-Nicalon Type S fiber, the effect of increasing fiber volume to increase the thermal diffusivity was positive if a matrix thermal conductivity value of 5 $W\,m^{-1}\,K^{-1}$ was used but negative if a matrix thermal conductivity value of 15 $W\,m^{-1}\,K^{-1}$ was used.

The present calculations indicate that when the matrix thermal conductivity has a low value due to low density and high porosity, highly thermal conductive SiC fiber strongly increases the composite thermal conductivity. Increasing total fiber volume is beneficial since both Z- and XY-directions of high thermal conductive SiC fiber are found contributory although the Z-directional one is more effective for increasing through-the-thickness thermal diffusivity. For the case of high thermal conductive matrix, highly thermal conductive SiC fiber seems to play a secondary role. Hence, achieving higher matrix density is more important than increasing the fiber volume as far as the means for increasing composite thermal conductivity. When using low thermal conductive SiC fiber in high thermal conductive matrix, the composite thermal diffusivity will be significantly reduced.

Finally, it should be mentioned that when carbon interface between fiber and matrix existed, the interface reduced thermal diffusivity/conductivity transverse to

Table 2
Density and thermal conductivity for fibers and matrixes

	Tyrrano SA fiber [9,10]	Hi-Nicalon Type S [14]	Hi-Nicalon [14]	CVI matrix[a]	PIP matrix[a]	
Density ($g\,cm^{-3}$)	3.02	3.10	2.74	2.8	2.38	2.10
Thermal conductivity	60 (RT)	18.5	8	67	22	10
($W\,m^{-1}\,K^{-1}$)	34 (600 °C)	16	10	37	15	5

[a] Matrix densities were estimated from measured bulk density of composite, fiber density, and fiber volume. For CVI matrix thermal conductivity, CVD SiC values supplied by Mitsui Engineering were adopted. For PIP, the values were assumed for the FEM calculations.

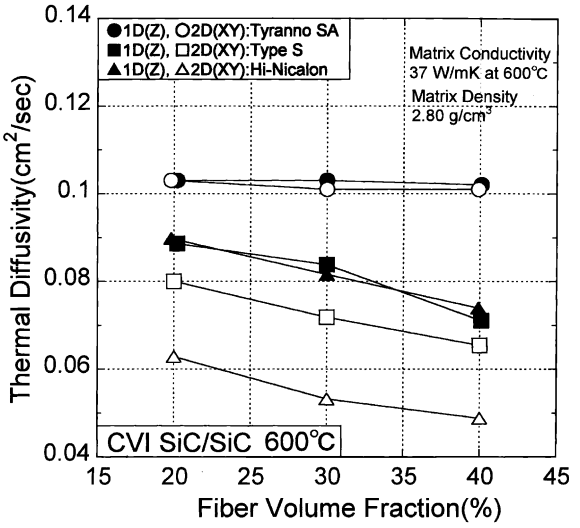

Fig. 5. Calculated results of through-the-thickness thermal diffusivity at 600 °C for 1D and 2D CVI SiC/SiC composites vs. fiber volume made with three different fibers (Tyranno SA, Hi-Nicalon, and Hi-Nicalon Type S).

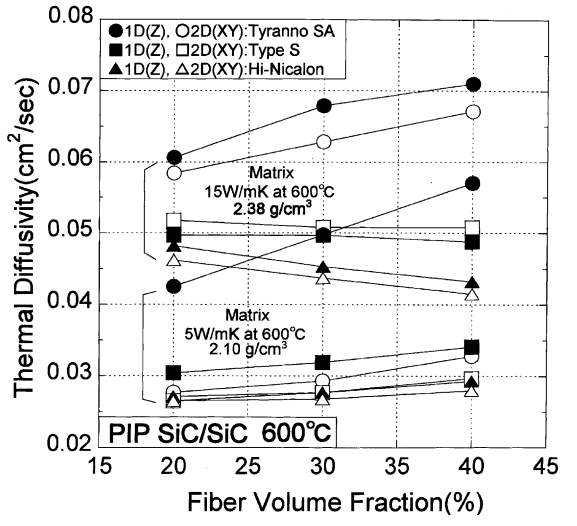

Fig. 6. Calculated results of through-the-thickness thermal diffusivity at 600 °C for 1D and 2D PIP SiC/SiC composites vs. fiber volume made with three different fibers (Tyranno SA, Hi-Nicalon, and Hi-Nicalon Type S). Two different matrix thermal conductivities and matrix densities were used for input data as noted in the figure.

the fiber direction mainly due to the imperfect interfacial thermal contact [16–18]. If there were carbon interface, the effectiveness of X- and Y-directions of highly thermal conductive SiC fiber to increase the through-the-thickness thermal conductivity would be much more reduced than that of Z-direction.

5. Summary and conclusions

The thermal diffusivity/conductivity for 3D-CVI and PIP SiC/SiC composites was measured by the thermal flash diffusivity method. For their 3D-SiC fabric preforms, Tyranno SAC, which were made by weaving amorphous Si–Al–C–O fiber and followed by sintering at a high temperature over 1900 °C, were used with three types of fiber configurations $X{:}Y{:}Z = 1{:}1{:}0.2$, 1:1:1, 1:1:4. The CVI and PIP SiC/SiC composites exhibited relatively high values, about 60 and 25 $\mathrm{W\,m^{-1}\,K^{-1}}$ at room temperature, respectively, and around 25 and 15 $\mathrm{W\,m^{-1}\,K^{-1}}$ at 1000 °C, respectively.

2D-FEM thermal analysis was performed to simulate laser flash thermal diffusivity measurement. In the analysis, SiC fiber volume and configuration as well as matrix porosity were taken into account. The agreement between the FEM results and experimental results was fairly good for CVI composites where the matrix had a relatively high thermal conductivity and density. Rectangular cavities were introduced into the matrix region to simulate the effect of porosity on the reduction of the composite thermal conductivity. Better results were obtained by adding this correction for PIP composites.

The FEM calculations for 1D and 2D composites reveal that highly thermal conductive SiC fiber can increase composite thermal diffusivity much more effectively when the matrix thermal conductivity is smaller. Therefore, the use of highly thermal conductive SiC fiber is quite beneficial for PIP composites for improving their thermal properties. In contrast, low thermal conductive SiC fibers significantly decrease the composite thermal diffusivity with increasing fiber volume when the matrix conductivity is high, such as the cases of CVI or reaction sintering/bonding.

References

[1] S. Nishio, S. Ueda, I. Aoki, R. Kurihara, T. Kuroda, H. Miura, T. Kunugi, Y. Seki, T. Nagashima, M. Ohara, J. Adachi, S. Yamazaki, I. Kawaguchi, T. Hashimoto, K. Shinya, Y. Murakami, H. Takase, T. Nakamura, Fus. Eng. Des. 41 (1998) 357.
[2] S. Ueda, S. Nishio, Y. Seki, R. Kurihara, J. Adachi, S. Yamazaki, DREAM design team, J. Nucl. Mater. 258–263 (1998) 1589.
[3] L.L. Snead, R.H. Jones, A. Kohyama, P. Fenici, J. Nucl. Mater. 233–237 (1996) 26.
[4] A. Hasegawa, A. Kohyama, R.H. Jones, L.L. Snead, B. Riccardi, P. Fenici, J. Nucl. Mater. 283–287 (2000) 128.
[5] D.J. Senor, G.E. Youngblood, C.E. Moore, D.J. Trimble, G.A. Newsome, J.J. Woods, Fus. Technol. 30 (1996) 943.
[6] R.H. Jones, D. Steiner, H.L. Heinisch, G.A. Newsome, H.M. Kerch, J. Nucl. Mater. 245 (1997) 87.
[7] R. Yamada, T. Taguchi, N. Igawa, J. Nucl. Mater. 283–287 (2000) 574.

[8] T. Ishikawa, Y. Kohtoku, K. Kumagawa, T. Yamamura, T. Nagasawa, Nature 391 (1998) 773.
[9] T. Nakayasu, M. Sato, T. Yamamura, K. Okamura, Y. Katoh, A. Kohayama, Ceram. Eng. Sci. Proc. 20 (4) (1999) 301.
[10] T. Ishikawa, S. Kajii, T. Hisayuki, Ceram. Eng. Sci. Proc. 21 (4) (2000) 323.
[11] T. Ishikawa, S. Kajii, K. Matsunaga, T. Hogami, Y. Kohtoku, T. Nagasawa, Science 282 (1998) 1295.
[12] W.J. Parker, R.J. Jenkins, C.P. Butler, G.L. Abbott, J. Appl. Phys. 32 (1961) 1679.
[13] Specific heat, nonmetalic solids, in: Y.S. Touloukian, E.H. Buyco (Eds.), Thermophysical Properties of Matter, The TPRC Data Series, vol. 5, IFI/Plenum, New York, 1970, p. 448.
[14] A. Urano, J. Sakamoto, M. Takeda, Y. Imai, H. Araki, T. Noda, Ceram. Eng. Sci. Proc. 19 (3) (1998) 55.
[15] R. Yamada, T. Taguchi, J. Nakano, N. Igawa, Ceram. Eng. Sci. Proc. 20 (3) (1999) 273.
[16] H. Bhatt, K.Y. Donaldson, D.P.H. Hasselman, R.T. Bhatt, J. Am. Ceram. Soc. 75 (1992) 334.
[17] C.-W. Nan, X.-P. Li, R. Birringer, J. Am. Ceram. Soc. 83 (2000) 848.
[18] G.E. Youngblood, D.J. Senor, R.H. Jones, these Proceedings.